Cancer Imaging

International Edition: DOI: 10.1002/anie.201601744
German Edition: DOI: 10.1002/ange.201601744

Bioorthogonal Turn-On Probe Based on Aggregation-Induced Emission Characteristics for Cancer Cell Imaging and Ablation

*Youyong Yuan[+], Shidang Xu[+], Xiamin Cheng, Xiaolei Cai, and Bin Liu**

Abstract: *Bioorthogonal turn-on probes have been widely utilized in visualizing various biological processes. Most of the currently available bioorthogonal turn-on probes are blue or green emissive fluorophores with azide or tetrazine as functional groups. Herein, we present an alternative strategy of designing bioorthogonal turn-on probes based on red-emissive fluorogens with aggregation-induced emission characteristics (AIEgens). The probe is water soluble and non-fluorescent due to the dissipation of energy through free molecular motion of the AIEgen, but the fluorescence is immediately turned on upon click reaction with azide-functionalized glycans on cancer cell surface. The fluorescence turn-on is ascribed to the restriction of molecular motion of AIEgen, which populates the radiative decay channel. Moreover, the AIEgen can generate reactive oxygen species (ROS) upon visible light (λ = 400–700 nm) irradiation, demonstrating its dual role as an imaging and phototherapeutic agent.*

Bioorthogonal chemistry with selective covalent labeling of biomolecules in cells and living organisms have garnered much attention from both chemists and biologists.[1] In these labeling reactions, one functional group is first incorporated into target biomolecules via metabolic or genetic approaches.[2] Subsequently, an exogenous fluorescent probe functionalized with a complementary group is introduced and covalently linked to the target of interest through click reaction, allowing for specific analyte detection.[3] Among them, fluorescence turn-on probes whose emission increases upon click reaction is more attractive due to their low background signal and high signal output.[4] Several elegant bioorthogonal turn-on probes utilizing azide- or tetrazine-functionalized fluorophores have been developed for biomolecular imaging.[5] Majority of the tetrazine based probes are based on fluorophores with blue or green emission.[5b–d] Recently, fluorogenic azide probes with longer absorption and emission wavelengths have been realized.[5e–h] As the diversity of bioorthogonal labeling is highly dependent on the novel labeling reagents, it is thus of great interest to further explore new strategies to design bioorthogonal turn-on probes. Over the past years, bioorthogonal chemistry has also been utilized for cancer targeting and ablation.[6] Traditional targeting strategies relying on biological interaction have been reported to face the problem of heterogeneity of cancer cells or saturation of receptors.[7] Bioorthogonal conjugation has emerged as an attractive alternative to biological interaction. Through metabolic approaches, unnatural targets with functional groups can be artificially introduced to specific cancer cells to achieve targeting through bioorthogonal conjugation.[6] These systems are based on bioorthogonal group modified nanoparticles which may reduce their reactivity due to steric hindrance. It is of great interest if one could develop a single bioorthogonal turn-on probe with dual role of imaging and therapy, which is not available yet. Recently, fluorogens with aggregation-induced emission characteristics (AIEgens) have received great attention in both fundamental study and practical applications.[8] Distinctive to traditional fluorogens that show a notorious phenomenon known as aggregation caused quenching (ACQ),[9] AIEgens are non-emissive in molecularly dissolved state but can be induced to emit strongly in aggregated state due to the restriction of intramolecular motions and prohibition of energy dissipation via non-radiative channels.[8a] The unique feature of AIEgens has opened new opportunities to develop ultra-bright organic dots[8a] and fluorescent light-up probes[8b] for sensing and bioimaging. Recently, AIEgens with efficient ROS generation have also been developed to serve as phototherapeutic agents for image-guided cancer cell ablation.[10]

In this contribution, as a proof of concept, we present for the first time an alternative strategy to design bioorthogonal

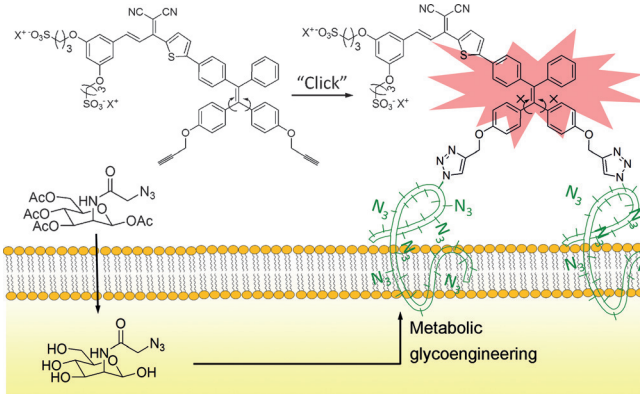

Scheme 1. Bioorthogonal turn-on probe TPETSAI for cancer cell imaging.

[*] Dr. Y. Yuan,[+] S. Xu,[+] Dr. X. Cheng, X. Cai, Prof. B. Liu
Department of Chemical and Biomolecular Engineering
National University of Singapore
4 Engineering Drive 4, Singapore 117585 (Singapore)
E-mail: cheliub@nus.edu.sg
Prof. B. Liu
Institute of Materials Research and Engineering
Agency for Science, Technology and Research (A*STAR)
3 Research Link, Singapore, 117602 (Singapore)
[+] These authors contributed equally to this work.

Supporting information for this article can be found under: http://dx.doi.org/10.1002/anie.201601744.

fluorescence turn-on probes based on AIEgens (Scheme 1). The probe is almost non-fluorescent in aqueous media but it displays significant fluorescence turn-on upon the restriction of molecular motion of the AIEgen through bioorthogonal reaction, enabling sensitive cancer cell imaging. Moreover, the specially designed AIEgen can also generate ROS upon visible light ($\lambda = 400$–700 nm) irradiation, implying dual action as an imaging and phototherapeutic agent for image-guided cancer cell ablation.

Tetraphenylene (TPE) is the iconic AIEgen which is very easy to modify.[8a] The synthetic route to the TPE derivatives of TPETS and TPETSAl is shown in Scheme 2. Suzuki

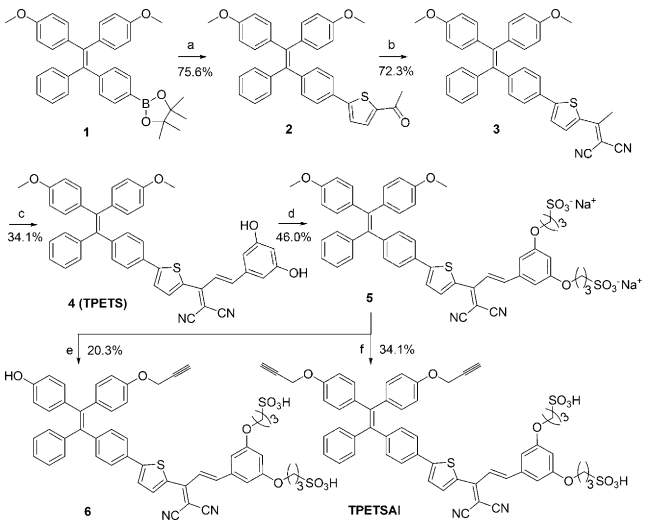

Scheme 2. Synthetic route to TPETS and TPETSAl. Reagents: a) tetrakis(triphenylphosphine)palladium(0), K_2CO_3, 4-acetyl-5-bromothiophene; b) malononitrile, ammonium acetate, silica gel; c) 3,5-dihydroxybenzaldehyde, piperidine, 2-propanol; d) 1,3-propanesultone, sodium methoxide; e, f) hydrobromic acid, then propargyl toluene-4-sulfonate (1 equiv. for (e), 5 equiv. for (f)), K_2CO_3, methanol, HPLC.

reaction between compound **1**[10] and 2-acetyl-5-bromothiophene yielded the intermediate compound **2**, which was further reacted with malononitrile to produce compound **3**. Further treatment of compound **3** with 3,5-dihydroxybenzaldehyde in the presence of piperidine yielded compound **4** (TPETS), which reacted with 1,3-propanesultone to afford compound **5**. The methoxy groups of compound **5** were deprotected and further functionalized with alkyne groups to offer the probe of TPETSAl and the compound **6**. The probe and the intermediates were well characterized (Figures S1–S7 in the Supporting Information). The absorption of TPETSAl and compound **6** lies in the visible region with a strong absorbance at 480 nm (Figure S8), which could be directly excited by the 488 nm laser equipped on the confocal microscope.

We first studied the optical properties of TPETS and TPETSAl. The PL spectra of TPETS in tetrahydrofuran (THF) and water mixtures with different water fractions (f_{water}) are shown in Figure S9A. TPETS is almost non-fluorescent in its benign solvent (THF), which is attributed to the easy molecular motion in molecularly dissolved state. However, with the increse of water (poor solvent) fractions, TPETS shows intense fluorescence in the far-red region. At the f_{water} of 99%, the PL intensity is 200-fold stronger than that in THF. The fluorescence enhancement should be due to the restriction of intramolecular motion,[8a] as TPETS tends to aggregate when f_{water} is increased. The aggregation formation of TPETS was confirmed by laser light scattering (LLS) study and transmission electron microscopy (TEM) image (Figure S10). Similarly, as shown in Figure S9B, the water soluble TPETSAl is almost non-emissive in water but it is highly fluorescent in its poor solvent (THF), confirming that TPETSAl is also AIE-active. The PL spectra of TPETS and TPETSAl were studied in DMSO/PBS buffer ($v/v = 1/99$). As shown in Figure 1A, TPETS is highly fluorescent while

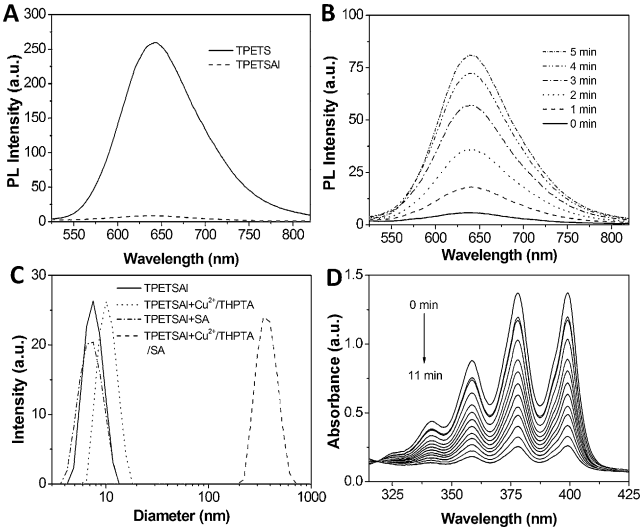

Figure 1. A) PL spectra of TPETS and TPETSAl in DMSO/PBS mixtures ($v/v = 1/99$). B, C) Time-dependent PL change (B) and size distributions (C) of TPETSAl (15 μM) upon click reaction with 1,3,5-tris(azidomethyl)benzene (10 μM) in the presence of $CuSO_4$/THPTA and sodium ascorbate (SA). For (A) and (B), the insets are the corresponding photographs taken under illumination of a UV lamp. D) The changes in absorption spectra for ABDA upon mixing with TPETSAl (10 μM) followed by white light irradiation at a power density of 100 mW cm^{-2}. Asc stands for ROS scavenger ascorbic acid (Asc).

TPETSAl fluoresces very weakly, which indicates that TPETSAl has extremely low background signal as designed. The PL intensity of the probe remains weak in aqueous solution with different ionic strength or different proteins (Figure S11). It should be noted that compound **6** shows similar photophysical properties to TPETSAl.

To investigate the fluorescence turn-on of TPETSAl upon click reaction, we adopted an $A_2 + B_3$ reaction using 1,3,5-tris(azidomethyl)benzene (B_3) as a model azide to form the cross-linked aggregates with TPETSAl (A_2). The click reaction was catalyzed by $CuSO_4$ with tris(3-hydroxypropyltriazolylmethyl) amine (THPTA) as ligand[11] and sodium ascorbate (SA) as reducing agent. The fluorescence changes were monitored, and the results are shown in Figure 1B. The fluorescence at 650 nm intensifies gradually with time and reaches a plateau in 5 min, which is 18-fold brighter than its

original emission. We further studied the underlying mechanism for the fluorescence turn-on. DLS studies revealed the formation of aggregates after the click reaction, which was verified by the changes in the average hydrodynamic diameters of TPETSAl, being less than 10 nm for TPETSAl to 300 nm after the click reaction (Figure 1C). Under the same conditions, the sole addition of $CuSO_4$ or SA resulted in negligible size changes. These results clearly demonstrate that the fluorescence change of TPETSAl upon click reaction is due to the formation of aggregates, which restrict the molecular motions. In contrast, the solution containing compound **6** and 1,3,5-tris(azidomethyl)benzene showed a negligible fluorescence change with no aggregate formation before and after the click reaction.

The ROS generation of TPETSAl upon visible light ($\lambda =$ 400–700 nm) irradiation was studied by using 9,10-anthracenediyl-bis(methylene)dimalonic acid (ABDA) as an indicator. As shown in Figure 1D, the absorption peaks at 325–400 nm are attributed to the anthracene moiety in ABDA. The absorbance decreases gradually upon light irradiation. However, the decrease was remarkably inhibited in the presence of ROS scavenger ascorbic acid (Asc), further confirming the ROS generation of TPETSAl upon light irradiation. As shown in Figure S12, the ROS generation quantum yield (Φ) of TPETSAl was determined to be 0.43 using Rose Bengal as the standard PS ($\Phi_{RB} = 0.75$ in water), which is similar to the clinically used PSs such as Photofrin ($\Phi = 0.28$) or Laserphyrin ($\Phi = 0.48$).[11]

To explore the potential of using TPETSAl for bimolecular imaging in live cells, human cervix carcinoma HeLa and breast cancer MDA-MB-231 cells were first incubated with peracetylated *N*-azidoacetylmannosamine (Ac_4ManNAz), which was taken up and incorporated into glycan with azide groups on cell surface through metabolic glycoengineering.[2] Subsequently, the labeling was performed with a cocktail containing 25 μM $CuSO_4$, 125 μM THPTA, 10 μM TPETSAl and 2.5 mM SA. The fluorescence of TPETSAl was studied by confocal image. THPTA used in this work can not only accelerate the click reaction but also endow the biocompatibility of click reaction.[12] The cell viabilities of Ac_4ManNAc pretreated HeLa cells incubated with $CuSO_4$ in the presence or absence of THPTA were studied. As shown in Figure S13, Ac_4ManNAz does not induce cell death, but $CuSO_4$ shows significant proliferation inhibition to both cell lines. However, in the presence of THPTA, the cells are alive up to the copper concentration of 50 μM. As shown in Figure 2A, strong red fluorescence can only be observed in the membrane of HeLa cells when incubated with TPETSAl in the presence of both Cu^{2+} and SA. When HeLa cells are treated with different concentrations of Ac_4ManNAz, the fluorescence shows a dose-dependent manner (Figure 2B). This dose-dependent expression of unnatural targets on cancer cells is very useful as the therapeutic agent can be artificially controlled by simply changing the amount of substrates. In addition, the effect of probe concentration on cell labeling was also studied. The results shown in Figure 2C clearly reveal the concentration-dependent fluorescence on the cell surface. It is also important to note that TPETSAl offers real-time labeling of metabolic glycoengineered HeLa cells. As shown in Figure 2D, the fluorescent signal of TPETSAl increases gradually as the click reaction progresses while the dark background further confirms the probe turn-on. When the click reaction was performed with compound **6** (the same concentration as TPETSAl) with Ac_4ManNAz pretreated HeLa cells, only dim fluorescence is observed (Figure S14). It should be noted that the control cells treated with peracetylated *N*-acetylmannosamine (Ac_4ManNAc) after click reaction with TPETSAl also showed negligible fluorescence (Figure S15). The mechanism for the fluorescence turn-on is thus mainly attributed to the restriction of free rotation of phenyl rings when both alkyne groups are clicked to the cell surface, although a single arm click also plays a minor role. The fluorescence change of TPETSAl after click reaction was also confirmed by flow cytometric analysis (Figure S16). Similar results were observed when performing the same experiments on MDA-MB-231 cells (Figure S17).

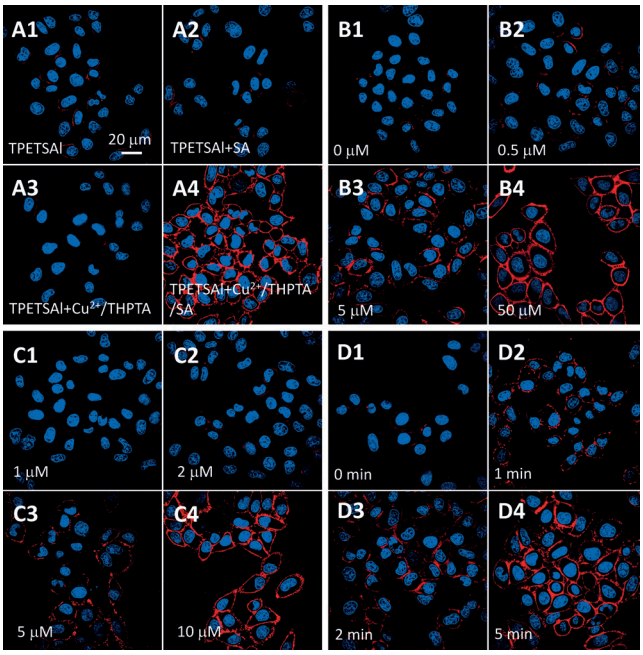

Figure 2. A) Confocal images of TPETSAl (10 μM) labeling on the Ac_4ManNAz (50 μM) pretreated HeLa cells with the addition of TPETSAl (A1), TPETSAl with SA (A2), TPETSAl with Cu^{2+}/THPTA (A3) or TPETSAl with Cu^{2+}/THPTA and SA (A4) for 5 min. The concentrations of Cu^{2+}, THPTA and SA are 25 μM, 125 μM and 2.5 mM, respectively. B) Confocal images of TPETSAl labeled HeLa cells pretreated with different concentrations of Ac_4ManNAz. C) Confocal images of Ac_4ManNAz (50 μM) pretreated HeLa cells labeled with different concentrations of TPETSAl. D) Time-dependent images of TPETSAl labeled HeLa cells by click reaction. Blue fluorescence (nucleus live dyed with Hoechst 33342, E_x: 405 nm, E_m: 430–470 nm); red fluorescence (TPETSAl, E_x: 488 nm, E_m: >650 nm).

The location of TPETSAl on cellular membrane was further confirmed by co-staining with a cell membrane tracker CellMask Green. As shown in Figure 3A, the red fluorescence from TPETSAl co-localizes well with the green fluorescence from CellMask Green, confirming that the probe is located on cell membrane. More importantly, TPETSAl with far-red emission enabled multicolor imaging with other well established probes for cellular organelles, such

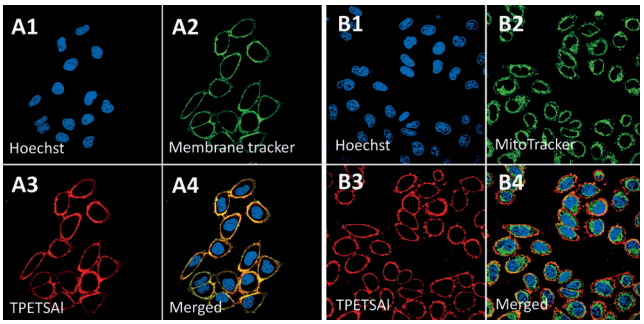

Figure 3. Co-stain of TPETSAI labeled HeLa cells with A) membrane tracker CellMask Green or B) MitoTracker Green. Blue fluorescence (nuclei live dyed with Hoechst 33342, E_x: 405 nm, E_m: 430–470 nm); green fluorescence (MitoTracker Green or CellMask Green, E_x: 488 nm; E_m: 505–525 nm); red fluorescence (TPETSAI, E_x: 488 nm, E_m: >650 nm).

as MitoTracker Green for mitochondrial stain and Hoescht 33342 for nuclear stain. As shown in Figure 3B, distinct cellular components were clearly visible in three colors, establishing the utility of TPETSAI for multicolor imaging.

The AIEgen used in this work can not only be used as an imaging agent but also as a therapeutic agent upon visible light ($\lambda = 400$–700 nm) irradiation. The fluorescence labeling of target cancer cells is particularly useful for phototherapy as light can be precisely applied onto the pathological region, while leaving normal cells untouched. A prerequisite for phototherapy is that the phototherapeutic agent should exhibit low cytotoxicity in dark and is able to induce a high percentage of cell death upon exposure to light. The intracellular ROS generation and cell necrosis were confirmed by using 2′,7′-dichlorofluorescin diacetate (DCF-DA) and propidium iodide (PI) as indicators, respectively (Figure S18). It should also be noted that under the studied conditions the HeLa cells upon light irradiation can not induce ROS generation (Figure S18A). We next evaluated the viability of TPETSAI labeled cells in dark condition and found no significant cytotoxicity to HeLa and MDA-MB-231 cells (Figure 4A). However, when exposed to light irradiation, a dose-dependent cytotoxicity is observed (Figure 4B). The half-maximal inhibitory concentration (IC_{50}) to HeLa cells is 7.3 μM. The phototoxicity index, which is the ratio between the IC_{50} values in the dark and upon light irradiation, was calculated to be 33.1, indicating that TPETSAI is a good phototherapeutic agent.

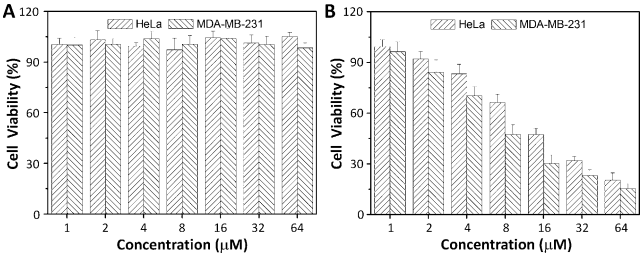

Figure 4. Viability of TPETSAI (10 μM) labeled HeLa and MDA-MB-231 cells A) in dark or B) with light irradiation for 2 min at a power density of 100 mW cm^{-2}.

In summary, we present a new strategy to design bioorthogonal turn-on probes for targeted cancer cell imaging and ablation. Thanks to the unique property of the AIEgens, the probe is very weakly fluorescent in aqueous media. However, upon click reaction to restrict the intramolecular motion, a strong red fluorescence is induced. The probe can be used for live-cell imaging of azide-functionalized glycans on metabolic glycoengineered cancer cells. Moreover, the probe is able to generate ROS upon light irradiation, which has been further used as a phototherapeutic agent. As compared to previously reported fluorogenic probes for bioorthogonal labeling and therapy, the red-emissive AIEgen represents a unique alternative for real-time live cell labeling, imaging and therapy. Next, we will focus on the development of AIEgen probes using copper-free click chemistry for in vivo labeling applications.

Acknowledgements

We thank the Ministry of Education (R279-000-391-112), Singapore NRF Investigatorship (R279-000-444-281) and the Institute of Materials Research and Engineering of Singapore (IMRE/14-8P1110) for financial support.

Keywords: aggregation-induced emission (AIE) · bioorthogonal probe · click chemistry · imaging · phototherapy

How to cite: *Angew. Chem. Int. Ed.* **2016**, *55*, 6457–6461
Angew. Chem. **2016**, *128*, 6567–6571

[1] a) E. M. Sletten, C. R. Bertozzi, *Angew. Chem. Int. Ed.* **2009**, *48*, 6974–6998; *Angew. Chem.* **2009**, *121*, 7108–7133; b) K. Lang, J. W. Chin, *Chem. Rev.* **2014**, *114*, 4764–4806.
[2] Z. Y. Hao, S. L. Hong, X. Chen, P. R. Chen, *Acc. Chem. Res.* **2011**, *44*, 742–751.
[3] a) A. Borrmann, J. C. M. van Hest, *Chem. Sci.* **2014**, *5*, 2123–2134; b) H. Jiang, B. P. English, R. B. Hazan, P. Wu, B. Ovryn, *Angew. Chem. Int. Ed.* **2015**, *54*, 1765–1769; *Angew. Chem.* **2015**, *127*, 1785–1789.
[4] J. Chan, S. C. Dodani, C. J. Chang, *Nat. Chem.* **2012**, *4*, 973–984.
[5] a) A. Nadler, C. Schultz, *Angew. Chem. Int. Ed.* **2013**, *52*, 2408–2410; *Angew. Chem.* **2013**, *125*, 2466–2469; b) L. G. Meimetis, J. C. Carlson, R. J. Giedt, R. H. Kohler, R. Weissleder, *Angew. Chem. Int. Ed.* **2014**, *53*, 7531–7534; *Angew. Chem.* **2014**, *126*, 7661–7664; c) H. Wu, J. Yang, J. Seckute, N. K. Devaraj, *Angew. Chem. Int. Ed.* **2014**, *53*, 5805–5809; *Angew. Chem.* **2014**, *126*, 5915–5919; d) Y. Chen, C. M. Clouthier, K. Tsao, M. Strmiskova, H. Lachance, J. W. Keillor, *Angew. Chem. Int. Ed.* **2014**, *53*, 13785–13788; *Angew. Chem.* **2014**, *126*, 14005–14008; e) J. J. Shie, Y. C. Liu, Y. M. Lee, C. Lim, J. M. Fang, C. H. Wong, *J. Am. Chem. Soc.* **2014**, *136*, 9953–9961; f) P. Shieh, V. T. Dien, B. J. Beahm, J. M. Castellano, T. Wyss-Coray, C. R. Bertozzi, *J. Am. Chem. Soc.* **2015**, *137*, 7145–7151; g) P. Agarwal, B. J. Beahm, P. Shieh, C. R. Bertozzi, *Angew. Chem. Int. Ed.* **2015**, *54*, 11504–11510; *Angew. Chem.* **2015**, *127*, 11666–11672; h) L. C.-C. Lee, J. C.-W. Lau, H.-W. Liu, K. K.-W. Lo, *Angew. Chem. Int. Ed.* **2016**, *55*, 1046–1049; *Angew. Chem.* **2016**, *128*, 1058–1061.
[6] a) H. Koo, S. Lee, J. H. Na, S. H. Kim, S. K. Hahn, K. Choi, I. C. Kwon, S. Y. Jeong, K. Kim, *Angew. Chem. Int. Ed.* **2012**, *51*, 11836–11840; *Angew. Chem.* **2012**, *124*, 12006–12010; b) L. Tang, Q. Yin, Y. X. Xu, Q. Zhou, K. M. Cai, J. Yen, L. W. Dobruckic, J. J. Cheng, *Chem. Sci.* **2015**, *6*, 2182–2186.

[7] R. Langer, *Nature* **1998**, *392*, 5 – 10.
[8] a) J. Mei, N. C. Leung, R. T. Kwok, J. Y. Lam, B. Z. Tang, *Chem. Rev.* **2015**, *115*, 11718 – 11940; b) J. Liang, B. Z. Tang, B. Liu, *Chem. Soc. Rev.* **2015**, *44*, 2798 – 2811; c) Y. Y. Yuan, C. J. Zhang, B. Liu, *Angew. Chem. Int. Ed.* **2015**, *54*, 11419 – 11423; *Angew. Chem.* **2015**, *127*, 11581 – 11585; d) Q. L. Hu, M. Gao, G. X. Feng, B. Liu, *Angew. Chem. Int. Ed.* **2014**, *53*, 14225 – 14229; *Angew. Chem.* **2014**, *126*, 14449 – 14453; e) A. D. Shao, Y. S. Xie, S. J. Zhu, Z. Q. Guo, S. Q. Zhu, J. Guo, P. Shi, T. D. James, H. Tian, W. H. Zhu, *Angew. Chem. Int. Ed.* **2015**, *54*, 7275 – 7280; *Angew. Chem.* **2015**, *127*, 7383 – 7388; f) Z. Xie, C. Chen, S. Xu, J. Li, Y. Zhang, S. Liu, J. Xu, Z. Chi, *Angew. Chem. Int. Ed.* **2015**, *54*, 7181 – 7184; *Angew. Chem.* **2015**, *127*, 7287 – 7290.
[9] J. B. Birks, *Photophysics of Aromatic Molecules*, Wiley, London, **1970**.
[10] a) F. Hu, Y. Y. Huang, G. X. Zhang, R. Zhao, H. Yang, D. Q. Zhang, *Anal. Chem.* **2014**, *86*, 7987 – 7995; b) Y. Y. Yuan, C. J. Zhang, M. Gao, R. Y. Zhang, B. Tang, B. Liu, *Angew. Chem. Int. Ed.* **2015**, *54*, 1780 – 1786; *Angew. Chem.* **2015**, *127*, 1800 – 1806; c) Y. Y. Yuan, C. Zhang, R. Kwok, S. Xu, R. Zhang, J. Wu, B. Z. Tang, B. Liu, *Adv. Funct. Mater.* **2015**, *25*, 6586 – 6595; d) S. Xu, Y. Yuan, X. Cai, C. Zhang, F. Hu, J. Liang, G. Zhang, D. Zhang, B. Liu, *Chem. Sci.* **2015**, *6*, 5824 – 5830.
[11] P. R. Ogilby, *Chem. Soc. Rev.* **2010**, *39*, 3181 – 3209.
[12] D. S. Amo, W. Wang, H. Jiang, C. Besanceney, A. C. Yan, M. Levy, Y. Liu, F. L. Marlow, P. Wu, *J. Am. Chem. Soc.* **2010**, *132*, 16893 – 16899.

Received: February 18, 2016
Published online: April 15, 2016

